Supplement of

Dynamic changes on Wilkins Ice Shelf during the 2006-2009 retreat derived from satellite observations

M. Rankl et al.

Correspondence to: Melanie Rankl (melanie.rankl@fau.de)

S1 SAR Data

Table S 1: Satellites and sensors used.

Intensity offset tracking

Sensor	Date	Rel. orbit/strip	Frame
ALOS PALSAR	18/09/2008	169	5680-5740
ALOS PALSAR	03/11/2008	169	5680-5740
ALOS PALSAR	22/10/2008	171	5680-5720
ALOS PALSAR	07/12/2008	171	5680-5720
ALOS PALSAR	28/09/2008	175	5680-5720
ALOS PALSAR	12/11/2008	175	5680-5720
ALOS PALSAR	15/05/2006	181	5670-5700
ALOS PALSAR	03/07/2006	181	5670-5700
ALOS PALSAR	14/06/2006	190	5650-5680
ALOS PALSAR	30/07/2006	190	5650-5680
ALOS PALSAR	09/06/2006	185	5650-5690
ALOS PALSAR	25/07/2006	185	5650-5690
ALOS PALSAR	26/06/2007	175	5670-5720
ALOS PALSAR	28/09/2007	167	5700-5730
ALOS PALSAR	11/11/2007	175	5670-5720
ALOS PALSAR	13/11/2007	167	5700-5730
ALOS PALSAR	20/10/2007	171	5680-5720
ALOS PALSAR	05/12/2007	171	5680-5720
ALOS PALSAR	21/09/2009	169	5700-5720
ALOS PALSAR	06/11/2009	169	5700-5720
ALOS PALSAR	09/09/2009	171	5690-5720
ALOS PALSAR	25/10/2009	171	5690-5720
ALOS PALSAR	01/10/2009	175	5680-5710
ALOS PALSAR	16/11/2009	175	5680-5710
ALOS PALSAR	09/10/2010	180	5650-5680
ALOS PALSAR	24/11/2010	180	5650-5680
ALOS PALSAR	09/08/2010	169	5700-5730
ALOS PALSAR	24/09/2010	169	5700-5730
ALOS PALSAR	29/09/2010	174	5670-5710
ALOS PALSAR	14/11/2010	174	5670-5710
ERS-1/2 SAR	02/03/1994	019	5728
ERS-1/2 SAR	17/03/1994	019	5728

ERS-1/-2 DInSAR

Sensor	Date	Rel. Orbit	Frame
ERS-1/2 SAR	23/10/1995	305	5715
ERS-1/2 SAR	24/10/1995	305	5715
ERS-1/2 SAR	11/03/1996	305	5715
ERS-1/2 SAR	12/03/1996	305	5715
ERS-1/2 SAR	08/03/1994	019	5715
ERS-1/2 SAR	11/03/1994	019	5715
ERS-1/2 SAR	03/03/1996	195	5085
ERS-1/2 SAR	04/03/1996	195	5085

S2 Intensity offset tracking

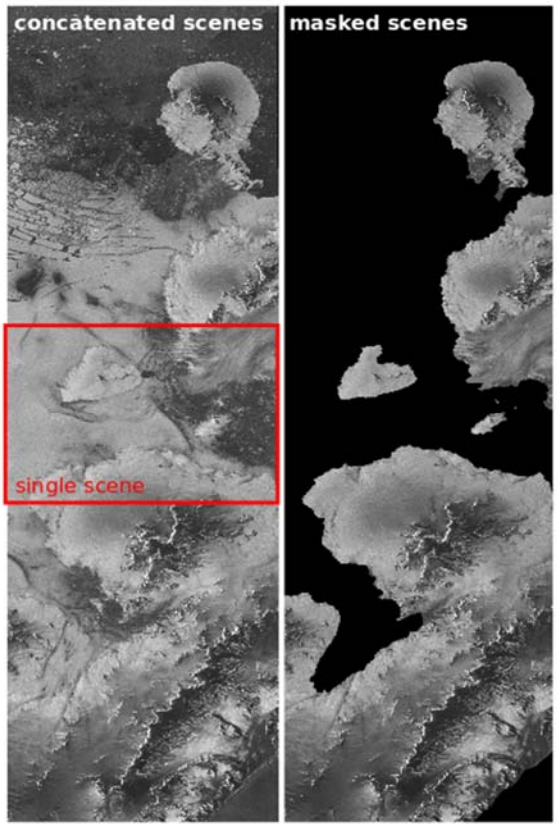

Figure S1: Example for concatenated and masked ALOS PALSAR SLC imagery.

S2.1 Error estimation of velocity products

The estimation of errors in the derived velocity products follows the method as described in Seehaus et al. (2015). The error estimation of the derived velocity fields consists of one term σ_v^C which describes uncertainties in the co-registration process. The magnitude of this term was derived from the median of stable points (up to 25000 samples per image pair) over ice rises, where zero ice motion is assumed. The second term σ_v^T describes uncertainties involved in the intensity tracking algorithm using

$$\sigma_v^T = \frac{C\Delta x}{z\Delta t} \quad \text{(Seehaus et al., 2015)}$$

Where C is the uncertainty of the tracking algorithm (C=0.4), Δx the image resolution in ground range, z the oversampling factor used in the tracking process and Δt the time period between image acquisitions. The final error estimate σ_v is derived from the sum of both term σ_v^C and σ_v^T.

Table S2: Error estimation of derived velocity fields.

date	sensor	σ_v^C	σ_v^T	σ_v
yyyy-mm-dd--yyyy-mm-dd		[m/d]	[m/d]	[m/d]
1994-03-02--1994-03-17	ERS SAR	0,0645311	0,2	0,2645311
2006-05-18--2006-07-03	PALSAR	0,0707297	0,03	0,1007297
2006-06-09--2006-07-25	PALSAR	0,249185	0,03	0,279185
2006-06-14--2006-07-30	PALSAR	0,267962	0,03	0,297962
2007-09-26--2007-11-11	PALSAR	0,25396	0,03	0,28396
2007-09-28--2007-11-13	PALSAR	0,1755955	0,03	0,2055955
2007-10-20--2007-12-05	PALSAR	0,0428592	0,03	0,0728592
2008-09-18--2008-11-03	PALSAR	0,186815	0,03	0,216815
2008-09-28--2008-11-13	PALSAR	0,113365	0,03	0,143365
2008-10-22--2008-12-07	PALSAR	0,037087	0,03	0,067087
2009-09-09--2009-10-25	PALSAR	0,06461115	0,03	0,09461115
2009-09-21--2009-11-06	PALSAR	0,0428839	0,03	0,0728839
2009-10-01--2009-11-16	PALSAR	0,1476365	0,03	0,1776365
2010-08-09--2010-09-24	PALSAR	0,04809755	0,03	0,07809755
2010-09-29--2010-11-14	PALSAR	0,0657041	0,03	0,0957041
2010-10-09--2010-11-24	PALSAR	0,08	0,03	0,11

S3 ERS-1/-2 Differential Interferometry

The location of the grounding zone was determined by using double differential SAR Interferometry (DInSAR) applied on ERS-1/-2 scenes (Fricker et al., 2009; Rignot, 1996; Rignot et al., 2011). During the ERS tandem phase (May 1995 to June 1996), both ERS satellites follow the same relative orbit with ERS-2 24 hours behind ERS-1 (Moore et al., 1999). This configuration allows for precise deformation measurements due to low spatial and temporal decorrelation of the signal. In order to extract the topographic phase information, we used 4-pass differential SAR interferometry (Rignot et al., 2011). The phase information of both interferograms contains vertical and horizontal displacements in range direction based on surface topography, ice flow, tidal motion, imaging geometry and noise (Rignot et al., 2011). By differencing the interferograms, the influence of the horizontal ice motion is removed, which is assumed to be constant between the image acquisitions. The vertical tidal signal, which is not constant over time, remains in the differential interferogram and allows to identify the grounding zone between grounded and floating ice of an ice shelf. The resulting differential interferogram contains an area of narrow fringes, which marks the flexure of the ice shelf plate and hence the dimension of the grounding zone (Figure S2). The differential interferogram was geocoded afterwards and the grounding line digitized based on the location of point G.

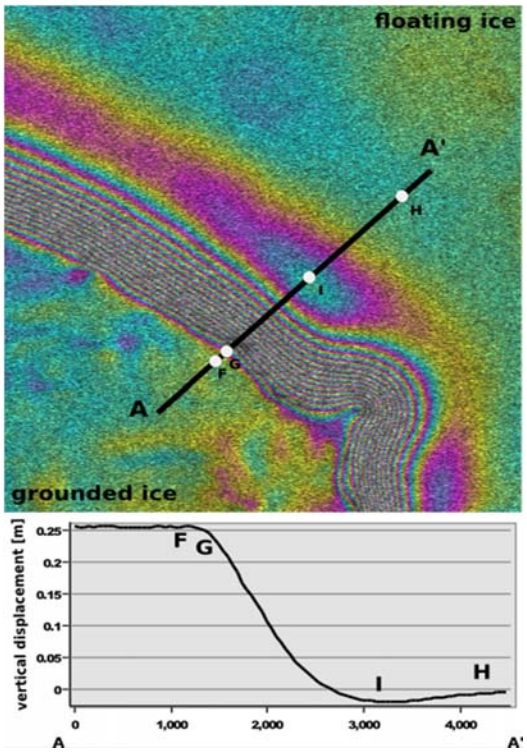

Figure S2: Grounding zone at Wilkins Ice Shelf: F: limit of tidal flexing, G: grounding line, I: local elevation minimum, H: maximum extent of flexure.

References

Fricker, H. A., Coleman, R., Padman, L., Scambos, T. A., Bohlander, J. and Brunt, K. M.: Mapping the grounding zone of the Amery Ice Shelf, East Antarctica using InSAR, MODIS and ICESat, Antarct. Sci., 21(5), 515–532, 2009.

Moore, P., Carnochan, S. and Walmsley, R. J.: Stability of ERS altimetry during the Tandem Mission, Geophys. Res. Lett., 26(3), 373–376, doi:10.1029/1998GL900313, 1999.

Rignot, E.: Tidal motion, ice velocity and melt rate of Petermann Gletscher, Greenland, measured from radar interferometry, J. Glaciol., 42(142), 1996.

Rignot, E., Mouginot, J. and Scheuchl, B.: Antarctic grounding line mapping from differential satellite radar interferometry, Geophys. Res. Lett., 38(10), 2011.

Seehaus, T., Marinsek, S., Helm, V., Skvarca, P. and Braun, M.: Changes in ice dynamics, elevation and mass discharge of Dinsmoor–Bombardier–Edgeworth glacier system, Antarctic Peninsula, Earth Planet. Sci. Lett., 427, 125–135, 2015.